Appl. Phys. B 49, 565–570 (1989)

Applied Physics B Photophysics and Laser Chemistry

Influence of End Reflectivity on Gain Saturation in a Planar Distributed Feedback Laser

P. Szczepański, D. Sikorski, and W. Woliński

Institute of Microelectronics and Optoelectronics, Technical University, ul. Koszykowa 75, PL-00-662 Warsaw, Poland

Received 3 April 1989/Accepted 3 June 1989

Abstract. An approximate method for the analysis of planar-waveguide distributed-feedback lasers is extended to include a nonvanishing reflectivity at the ends of the structure. An index grating structure with parasitic losses is investigated. An expression for the small-signal gain coefficient α_{0MN} as a function of the output power P_{MNout} normalized to the saturation power P_s, coupling coefficient κ, complex reflectivity $\mathscr{R}$ of end reflectors, and waveguide parameters is presented.

PACS: 42.60B, 42.60D, 42.80F, 42.80L

Distributed-feedback action was first demonstrated by Kogelnik and Shank [1, 2] in an active medium with index or gain modulation. Since these pioneering works [1, 2] the linear theory (see, for example, [3–6]) as well as nonlinear theory (see, for example, [7–10]) have been the subject of many publications.

By using only linear analysis, the eigenvalue equation for lasing frequencies and threshold gain characteristics can be derived. The nonlinear analysis [7–10] makes it possible to relate the power output to the laser parameters, but requires complicated computer calculations. Therefore, it is not very useful for the design process.

Haus has found [11] an approximate analytic formula describing the output power normalized to the saturation power as a function of the small signal gain coefficient, loss coefficient, and the coupling coefficient. The approximate analysis presented by Haus [11] has been developed in [12–14]. The results obtained are in good agreement with exact computer solutions [7, 8] for all regions of DFB laser operation that are likely to be of practical interest.

However, the above approximate analysis is developed for TEM waves. Thus, it cannot be applied directly for studying nonlinear operation of real distributed feedback lasers, where the waveguide effects have to be taken into consideration.

The first, an approximate analysis of waveguide DFB lasers have been presented for the planar structures in [15] and for the metal waveguides in [18]. In these studies the end reflectivity of the structures has been neglected. However, a more realistic description of DFB structures requires inclusion of the end reflectivity. It is especially difficult to give a complete and exact description of gain saturation with parasitic losses taking into account end reflectors (e.g., real structures), because of the large number of characteristic parameters and variables that are involved in the description and up to date this problem has not been studied.

The main purpose of our paper is to present an approximate analysis of the nonlinear operation of the planar DFB laser taking into account nonvanishing end reflectivity as well as waveguide effects. It provides a method of solution for this kind of the structures requiring only simple numerical calculations. Similarly, as we have done for bulk DFB structures [12–14] and for planar DFB structures [15] without end reflectivity, we have based our method on the energy approach by, using the appropriate threshold-field distribution of DFB laser in an exact energy theorem.

In the following section, we derive the approximate formula for the output power. The approximate formula obtained including end reflectivity is general and could be used for studying nonlinear operation of different planar DFB lasers. In order to compare results obtained for the structure with nonvanishing end reflectivity with those for the structure with zero

end reflectivity [15] we perform calculations for waveguide Nd lasers. Moreover, these kind of the lasers are potentially important for fiber-optics communication because of the relatively low loss of optical fibers at 1.06 μm. In addition, thin-film Nd lasers would be the most practical structures for possible integration with other passive thin-film optical elements and waveguides, which could be made of the Nd-laser host materials because of the low scattering and absorption losses at the Nd-laser wavelength. The conclusions are presented in Sect. 2.

1. Energy Relation for Planar Distributed-Feedback Structure

In order to compare the results obtained for a structure with end reflectors to the characteristics of a planar DFB waveguide laser with vanishing reflectivity, we use the same assumptions as in [15]. Thus, we confine our analysis to the index variation and envelope gain saturation of the active medium with no mode competition, since the characteristics of the planar DFB waveguide laser with vanishing reflectivity have been derived only with these assumptions [15].

An energy relation for a planar distributed feedback waveguide laser with index variation can be written in the following form [15]:

$$\frac{d}{dz}(|R_N|^2-|S_N|^2)=2(\alpha_N-\alpha_{ML})(|R_N|^2+|S_N|^2) -2[|R_N|^2\,\mathrm{Im}\{\xi_1\}+|S_N|^2\,\mathrm{Im}\{\xi_2\}]+S_NR_N^*\mathscr{U} +R_NS_N^*\mathscr{U}, \tag{1}$$

where

$$\mathscr{U}=-\mathrm{Im}\{\xi_2\}-\mathrm{Im}\{\xi_4\}+\mathrm{j}[\mathrm{Re}\{\xi_2\}-\mathrm{Re}\{\xi_4\}].$$

R_N and S_N are the complex amplitudes of two counter-running waves of the Nth longitudinal mode of the laser, α_{ML} is the loss coefficient taking into account scattering losses of the Mth laser mode at total reflection at the non-ideally smooth boundary surfaces of the waveguide. According to [16] the loss coefficient α_{ML} for TE modes is

$$\alpha_{ML}=2k_0^2\frac{(n_f^2-n_{effM}^2)^{3/2}}{n_{effM}} \times\frac{h_s^2+h_a^2}{t+1/(k_0\sqrt{n_{effM}^2-n_s^2})+1/(k_0\sqrt{n_{effM}^2-n_a^2})}, \tag{2}$$

where h_s and h_a are the mean peak-to-valley heights of the boundary surfaces, k_0 is the wave number in vacuum, n_{effM} is the effective index of the Mth waveguide mode and n_f, n_s, and n_a are the planar waveguide refractive indices (Fig. 1), t is the thickness of the unperturbed waveguide. The mode gain α_N may be

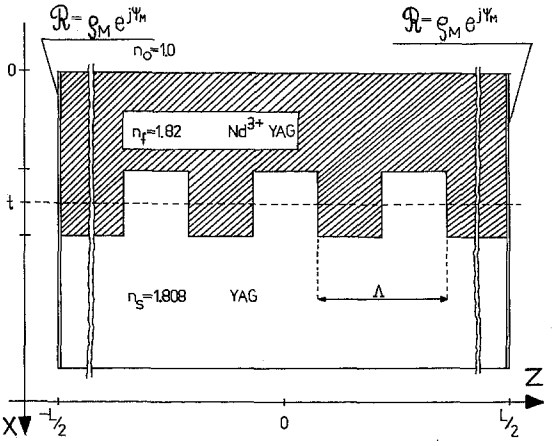

Fig. 1. A guided-wave DFB laser with end reflectors

written as

$$\alpha_{MN}=\frac{k_0}{2\beta_{0M}P}\int_{-\infty}^{\infty}dx\,n(x)(\hat{\alpha}-\alpha_{MNloss})\mathscr{E}_{0M}^2(x), \tag{3}$$

$$\beta_{0M}=k_0n_{effM},$$

where α_{MNloss} is the volume loss coefficient and $\mathscr{E}_{0M}^2(x)$ describes the transverse field distribution of the Mth waveguide mode in the periodic structure, β_{0M} is the propagation constant of the Mth waveguide mode, $n(x)$ describes the transverse index distribution and the normalization factor

$$P=\int_{-\infty}^{\infty}dx\,\mathscr{E}_{0M}^2(x). \tag{4}$$

The coupling coefficient is described by κ and in general, is a function of tooth shape. The complex constants ξ_i represent the reaction of all partial waves excited by R_N and S_N in periodic structure back on themselves. They are derived and discussed in more detail in [17].

For the homogeneous laser medium, when spatial hole burning effects and mode competition are disregarded, the gain coefficient $\hat{\alpha}$ can be written in terms of the small signal value α_{0MN} as

$$\hat{\alpha}=\frac{\alpha_{0MN}f(x,z)}{1+(|E_{RMN}|^2+|E_{SMN}|^2)/P_s}, \tag{5}$$

where $|E_{RMN}|^2+|E_{SMN}|^2$ describes the total power of the MNth mode in the structure, $f(x,z)$ describes spatial distribution of small signal gain in the medium and P_s is the saturation power. We assume that

$$E_{RMN}(x,z)=\mathscr{A}_{MN}\mathscr{E}_{0M}(x)\,R_N(z), \tag{6}$$

$$E_{SMN}(x,z)=\mathscr{A}_{MN}\mathscr{E}_{0M}(x)\,S_N(z), \tag{7}$$

where $\mathscr{A}_{MN}$, is a real amplitude of the MNth mode.

Because of the nonvanishing reflectivity at $z=\mp L/2$ where L is the length of the laser, we have new boundary conditions for the amplitudes of E_{RMN} and E_{SMN}. They can be written in the following form:

$$E_{\mathrm{RMN}}(x, z=-L/2)=\varrho_M e^{j\psi_M} E_{\mathrm{SMN}}(x, z=-L/2),$$

$$|1-\varrho_M e^{j\psi_M}|^2 \int_{-\infty}^{\infty} dx |E_{\mathrm{SMN}}(x, z=-L/2)|^2 = P_{\mathrm{SMNout}} \quad (8)$$

and

$$E_{\mathrm{SMN}}(x, z=L/2)=\varrho_M e^{j\psi_M} E_{\mathrm{RMN}}(x, z=L/2),$$

$$|1-\varrho_M e^{j\psi_M}|^2 \int_{-\infty}^{\infty} dx |E_{\mathrm{RMN}}(x, z=L/2)|^2 = P_{\mathrm{RMNout}}, \quad (9)$$

where $P_{\mathrm{SMNout}}+P_{\mathrm{RMNout}}=P_{\mathrm{MNout}}$ is the power of the MNth mode escaping at the ends of the structure and $\varrho_M e^{j\psi_M}=\mathscr{R}$ describes the complex reflectivity, ϱ_M is a real quantity and represents the amplitude reflectivity, which depends upon the transverse field distribution of the MNth mode i.e. depends on M number.

Using the boundary conditions (8, 9) and (6, 7) we can relate the amplitude $\mathscr{A}_{\mathrm{MN}}$ with the output power of the MNth mode. We can find that

$$|\mathscr{A}_{\mathrm{MN}}|^2 = \frac{P_{\mathrm{MNout}}}{P|1-\varrho_M e^{j\psi_M}|^2 [|R_N(L/2)|^2+|S_N(-L/2)|^2]}. \quad (10)$$

Integration of the energy relation (1) from $z=-L/2$ to $z=L/2$, while taking into account boundary conditions, (8, 9), gives

$$|1-\varrho_M e^{j\psi_M}|^2 [|R_N(L/2)|^2+|S_N(-L/2)|^2]$$
$$=2\int_{-L/2}^{L/2} (\alpha_{\mathrm{MN}}-\alpha_{\mathrm{ML}})(|R_N|^2+|S_N|^2)dz$$
$$-2\int_{-L/2}^{L/2} (|R_N|^2 \operatorname{Im}\{\xi_1\}+|S_N|^2 \operatorname{Im}\{\xi_3\})dz$$
$$+\mathscr{U}\int_{-L/2}^{L/2} S_N R_N^* dz+\mathscr{U}^* P\int_{-L/2}^{L/2} R_N S_N^* dz. \quad (11)$$

By application of (3, 5), we can rewrite relation (11) as follows:

$$\alpha_{0\mathrm{MN}}=\left\{r+2\int_{-L/2}^{L/2} dz\,\alpha_{\mathrm{ML}} f_N(z)-\mathscr{U}\int_{-L/2}^{L/2} dz S_N R_N^*-\mathscr{U}^*\int_{-L/2}^{L/2} dz S_N^* R_N\right.$$
$$\left.+2\int_{-L/2}^{L/2} dz f_N(z)\frac{k_0}{P\beta_{0M}}\int_{-\infty}^{\infty} dx\,\mathscr{E}_{0M}^2(x)\alpha_{\mathrm{MNloss}}+2\int_{-L/2}^{L/2} dz[|S_N|^2 \operatorname{Im}\{\xi_1\}+|R_N|^2 \operatorname{Im}\{\xi_2\}]\right\}$$
$$\times\left\{2\int_{-L/2}^{L/2} dz f_N(z)\frac{k_0}{P\beta_{0M}}\int_{-\infty}^{\infty} dx\,n(x)\mathscr{E}_{0M}^2(x)f(x,z)\Big/\left(1+\frac{P_{\mathrm{RMNout}}+P_{\mathrm{SMNout}}}{P_s}\frac{\mathscr{E}_{0M}^2(x)f_N(z)}{r}\right)\right\}^{-1}, \quad (12)$$

where $f_N(z)=|R_N|^2+|S_N|^2$ and $r=|1-\varrho_M e^{j\psi_M}|^2 f_N(z)$. This formula is exact and relates the small-signal gain in the medium to the output power and system parameters for a distributed feedback planar structure with end reflectors. It has a form similar to the energy relation for the small-signal gain coefficient presented in [15] yet it is more general, as it takes into account nonvanishing end reflectivity. We use it as the starting point for an approximate analysis.

Similarly, as it was done in [15], we confine our analysis to the case where the partial waves are neglected, i.e. $\xi_i=0$, and assume that R_N and S_N are proportional to the threshold field distribution for structure with end reflectors. Thus, according to [4], we have

$$R_N(z)=\sinh\gamma_N(z+L/2)\mp\varrho_M e^{j\psi_M}\sinh\gamma_N(z-L/2), \quad (13)$$

$$S_N(z)=\mp\sinh\gamma_N(z-L/2)+\varrho_M e^{j\psi_M}\sinh\gamma_N(z+L/2), \quad (14)$$

where the complex propagation constant γ_N is the solution of the eigenvalue equation

$$\gamma_N=\mp j\kappa\sinh\gamma_N L \times\frac{(1-\varrho_M e^{j2\psi_M})}{(1-\varrho_M e^{j\psi_M}e^{-\gamma_N L})(1\mp\varrho_M e^{j\psi_M}e^{\gamma_N L})} \quad (15)$$

and κ is the coupling coefficient. The upper sign applies to even modes and the lower to odd modes.

By using the threshold-field distribution (13, 14) for R_N and S_N and putting $\xi_i=0$ Eq. (12) can be rewritten for the normalized small signal gain $\alpha_{0\mathrm{MN}}L$, the normalized propagation constant $\gamma_N L=\Gamma_N$, and the normalized loss coefficient $\alpha_{\mathrm{ML}}L$ in the following form

$$\alpha_{0\mathrm{MN}}L=\left[r+2\int_{-1/2}^{1/2} d\xi\,\alpha_{\mathrm{ML}}L f_N(\xi)+2\int_{-1/2}^{1/2} d\xi f_N(\xi)\frac{k_0}{P\beta_{0M}}\int_{-\infty}^{\infty} dx\,\mathscr{E}_{0M}^2(x)\alpha_{\mathrm{MNloss}}L\right]$$
$$\left[2\int_{-1/2}^{1/2} d\xi f_N(\xi)\frac{k_0}{P\beta_{0M}}\int_{-\infty}^{\infty} dx\,n(x)\mathscr{E}_{0M}^2(x)f(x,\xi/L)\Big/\left(1+\frac{P_{\mathrm{RMNout}}+P_{\mathrm{SMNout}}}{P_s}\frac{\mathscr{E}_{0M}^2(x)f_N(z)}{r}\right)\right]^{-1}, \quad (16)$$

where

$f_N(\xi)=|\mathscr{R}_N|^2+|\varphi_N|^2$ and $r=|1-\varrho_M e^{j\psi_M}|^2 f_N(\xi)$,

and

$$\mathscr{R}_N(z)=\sinh\Gamma_N(\xi+1/2)\mp\varrho_M e^{j\psi_M}\sinh\Gamma_N(\xi-1/2), \quad (17)$$

$$\varphi_N(z)=\mp\sinh\Gamma_N(\xi-1/2)+\varrho_M e^{j\psi_M}\sinh\Gamma_N(z+1/2). \quad (18)$$

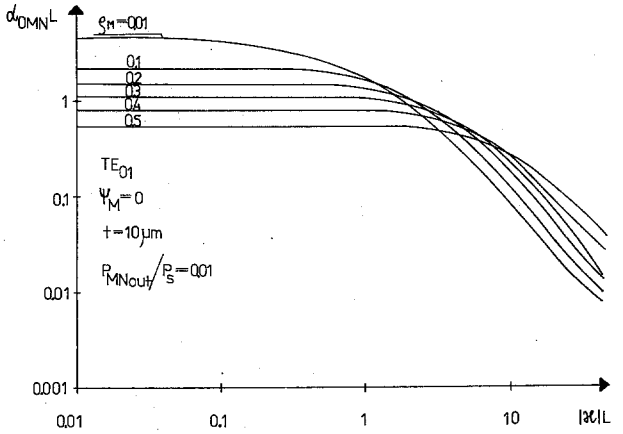

Fig. 2. Normalized small signal gain of the TE_{01} mode vs normalized coupling coefficient, with the amplitude reflectivity ϱ_M as a parameter. The normalized output power is $P_{MNout}/P_s = 0.01$, the thickness of the waveguide is $t = 10\ \mu m$, and phase of the complex reflectivity $\mathscr{R}$ is $\psi_M = 0$

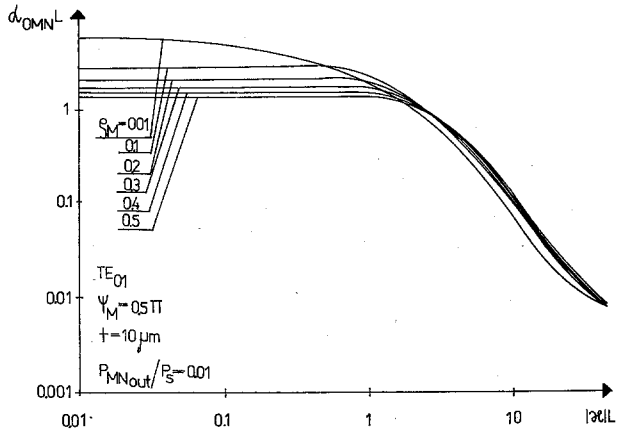

Fig. 3. Normalized small signal gain of the TE_{01} mode as a function of the normalized coupling coefficient, with ϱ_M as a parameter for $P_{MNout}/P_s = 0.01$, $t = 10\ \mu m$ and $\psi_M = \Pi/2$

Equation (16) is an approximate expression relating the normalized small-signal gain coefficient $\alpha_{0MN}L$ to system parameters. We use it to derive the characteristics of a planar DFB laser with end reflectors.

The plots of Figs. 2–6 are obtained by the approximate relation (16). Calculations are performed for an appropriate transverse field distribution $\mathscr{E}_{0M}(x)$ of the unperturbed planar structure with thickness t for which the zero-order Fourier coefficient of a Fourier series of the grating expansion vanishes. Since the volume losses α_{MNloss} are negligible compared with scattering losses α_{ML} we take into consideration only α_{ML} in our calculations. The data of the scattering losses for each thin-film thickness and given transverse mode number are obtained by (2) for the mean peak-to-valley heights of the boundary surfaces $h_a = h_s = 0.01\ \mu m$.

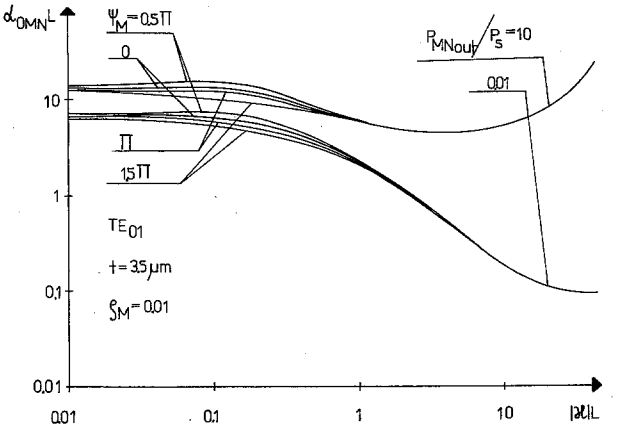

Fig. 4. Normalized small signal gain of the TE_{01} mode plotted against the normalized coupling coefficient, with ψ_M as a parameter, for two levels of the normalized output power, $P_{MNout}/P_s = 0.01$ and $P_{MNout}/P_s = 10$, the amplitude reflectivity $\varrho_M = 0.01$, and thickness of the waveguide $t = 3.5\ \mu m$

In Fig. 2 the normalized small signal gain $\alpha_{0MN}L$ is plotted versus the normalized coupling coefficient $|\kappa|L$ with the amplitude reflectivity ϱ_M, as parameter, for the normalized output power $P_{MNout}/P_s = 0.01$, the thickness of the waveguide $t = 10\ \mu m$ and the phase of the complex reflectivity $\mathscr{R}$, $\psi_M = 0$. For small values of the coupling coefficient the feedback mechanism is caused by the Fabry-Perot resonator. Thus, in this region of operation, when the amplitude reflectivity increases the small-signal gain required for given output power level decreases. For large coupling strength we observe a different behaviour of the characteristics. In this region of operation the distributed feedback mechanism dominates. An increase of the amplitude reflectivity causes an increase of the small-signal gain because of the strong competition for this phase of the complex reflectivity between Fabry-Perot and DFB modes.

When the phase of the complex reflectivity is changed, (Fig. 3), we observe a for small coupling coefficient similar behaviour of characteristics as for $\psi_M = 0$. But for large coupling strength the small-signal gain is not sensitive to the amplitude reflectivity, and characteristics for increasing $|\kappa|L$ tend towards the similar characteristics of structure without end reflectors.

Competition between the feedback mechanism caused by the mirror resonator and the feedback mechanism of the index grating is also observable in Fig. 4. In this figure the signal gain $\alpha_{0MN}L$ of the TE_{01} mode is plotted as a function of $|\kappa|L$ for four values of the phase ψ_M. The results are obtained for two levels of the output power, $P_{MNout}/P_s = 0.01$ and $P_{MNout}/P_s = 10$, $\varrho_M = 0.01$, and the thickness $t = 3.5\ \mu m$ of the waveguide near cutoff of the TE_{1N} modes, below this point. The characteristics presented in Fig. 4 are more sensi-

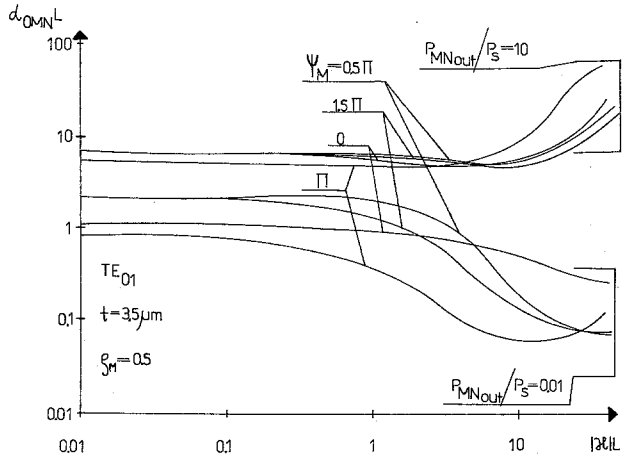

Fig. 5. Normalized small signal gain coefficient of the TE_{01} mode vs normalized coupling coefficient, with phase of the complex reflectivity as a parameter, for two levels of the normalized output power, $P_{MNout}/P_s=0.01$ and $P_{MNout}/P_s=10$, the amplitude reflectivity $\varrho_M=0.5$, and the thickness of the waveguide $t=3.5$ μm

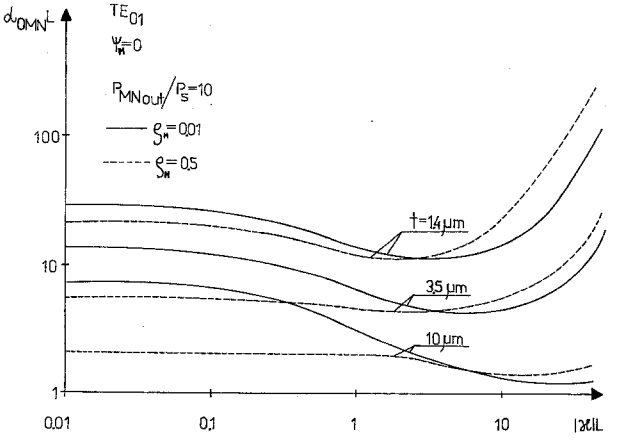

Fig. 6. Normalized small signal gain of the TE_{01} mode as a function of the normalized coupling coefficient, with thickness of the waveguide as a parameter, for two values of the amplitude reflectivity, $\varrho_M=0.01$ and $\varrho_M=0.5$ and phase of the complex reflectivity, $\psi_M=0$

tive to the phase ψ_M for coupling coefficients. For example, the maximum difference between the curves plotted for various phases is for $|\kappa|L\cong 0.1$. For this coupling coefficient both feedback mechanisms act with the same strength. We also notice that for a high output-power level the small-signal gain is less sensitive to the coupling coefficient.

Figure 5, shows a similar dependence for the amplitude reflectivity $\varrho_M=0.5$. In this case the characteristics strongly depend upon the phase ψ_M of the complex reflectivity $\mathscr{R}$. Note that for a high output power level, $P_{MNout}/P_s=10$ curves go through their minima within the given range of $|\kappa|L$. Thus, for each phase of the complex reflectivity and given thickness of the waveguide there exists an optimum coupling strength that results in the minimum small-signal gain required to maintain that power. For $P_{MNout}/P_s=0.01$ only the curve for $\psi_M=\Pi$ passes through its minimum. For other phases minima are shifted towards large coupling strengths that are out of the range shown for the coupling coefficient.

In Fig. 6, the normalized gain coefficient of the TE_{01} mode is plotted against the normalized coupling coefficient, with thickness of the waveguide as a parameter. The results are obtained for two values of the amplitude reflectivity, $\varrho_M=0.01$ and $\varrho_M=0.5$ and the phase $\psi_M=0$ of the complex reflectivity. Note that all curves shown in Fig. 6 go through a minimum within the range of the $|\kappa|L$ shown. When the thickness of the waveguide increases the value of the optimum coupling coefficient related to the minimum value of the small-signal gain increases. In addition, a competition between the feedback mechanism of the index grating and the feedback mechanism caused by mirror resonator can be observed. Firstly, when the normalized coupling coefficient increases the small-signal gain for $\varrho_M=0$ is less then the small-signal gain for $\varrho_M=0.01$ required to maintain the same output-power level. In this region of operation the feedback mechanism of the mirror resonator dominates. For the "critical" coupling which is a function of the thickness of the waveguide the small-signal-gain coefficient is equal for both amplitude reflectivities. For large coupling strength the small-signal-gain coefficient for $\varrho_M=0.01$ is less then the small signal gain for $\varrho_M=0.5$ required to maintain the same output power. In this region of operation the distributed feedback mechanism dominates, and an increase of the amplitude reflectivity causes an increase of the competition between DFB modes and Fabry-Perot modes. This results in the increase of the small-signal gain required to maintain a given output-power level.

2. Conclusions

In this paper we present an approximate method of analysis of nonlinear operation of the planar-waveguide distributed feedback laser with end reflectors. An approximate formula for normalized small-signal-gain coefficient $\alpha_{0MN}L$ as a function of system parameters, taking into account waveguide effects as well as end reflectivity, is obtained.

The characteristics presented in this paper show a strong influence of the amplitude reflectivity and phase of the complex reflectivity on operation of the planar waveguide DFB lasers. Competition between the feedback mechanism caused by the mirror resonator and the feedback mechanism of the index grating is observed. Also we find that for each value of system

parameters, i.e. the amplitude reflectivity, phase of the complex reflectivity, thickness of the waveguide and output power level, an optimal value exists of the coupling coefficient which is related to with the minimal value of the small-signal gain required to obtain a given output power level.

In order to compare characteristics of planar waveguide DFB lasers with and without end reflectors [15] calculations have been performed for the waveguide DFB Nd laser. However, the approximate formula presented in this paper is general and can be used for studying nonlinear operation of different planar DFB lasers with end reflectors, e.g., injection lasers.

Since it is difficult to give a complete description of gain saturation of such lasers by an exact computer solution of the corresponding nonlinear equations because of large number of parameters and variables, we are convinced that the presented technique facilitates the design of real structures and calculation of the optimal coupling strength for distributed feedback planar devices with nonvanishing end reflectivity.

Acknowledgements. The authors express their thanks to Prof. A. Kujawski for helpful discussion and valuable suggestions. This work has been supported by C.P.B.R.8.14.

References

1. H. Kogelnik, C.V. Shank: Appl. Phys. Lett. **18**, 52–154 (1971)
2. H. Kogelnik, C.V. Shank: J. Appl. Phys. **43**, 2327–2335 (1971)
3. S. Wang: IEEE J. QE-**10**, 414–427 (1974)
4. S.R. Chinn: IEEE J. QE-**9**, 574–580 (1973)
5. W. Streifer, D.R. Scifres, R.D. Burnham: J. Appl. Phys. **46**, 247–249 (1975)
6. S. Gnepf, F.K. Kneubühl: Theory on distributed feedback lasers with weak and strong modulation, in *Infrared and Millimeter Waves*, **16**, Chap. 2 (Academic, New York 1986) and references
7. K.O. Hill, A. Watanabe: Appl. Opt. **14**, 950–961 (1975)
8. K.O. Hill, R.T. MacDonald: IEEE J. QE-**12**, 716–721 (1976)
9. M. Sargent III, W.H. Swantner, J.D. Thomas: IEEE J. QE-**16**, 465–472 (1980)
10. P. Szczepański: IEEE J. QE-**24**, 1248–1257 (1988)
11. H.A. Haus: Appl. Opt. **14**, 2650–2652 (1975)
12. P. Szczepański: Appl. Opt. **24**, 2574–3578 (1985)
13. P. Szczepański: IEEE J. QE-**22**, 517–519 (1986)
14. P. Szczepański: J. Appl. Phys. **63**, 4854–4859 (1988)
15. P. Szczepański, D. Sikorski, W. Woliński: IEEE J. QE (in press)
16. P. Mockel, R. Platner, W. Kruhler, R. Reichelt, J. Grambmaier: Siemens Forsch.- u. Entwickl.-Ber. **5**, 287–295 and 296–302 (1976)
17. W. Streifer, D.R. Scifres, R.D. Burnham: IEEE J. QE-**13**, 134–141 (1977)
18. P. Szczepański, J. Arnesson, F.K. Kneubühl: Appl. Phys. B (in press)